

# Thrust Performance of Electromagnetic Acceleration Mode for Laser-Electric Hybrid Thrusters

IEPC-2007-56

*Presented at the 30<sup>th</sup> International Electric Propulsion Conference, Florence, Italy  
September 17-20, 2007*

Yusuke Sasaki\* and Hideyuki Horisawa†  
*Tokai University, Hiratsuka-shi, Kanagawa, 259-1292, Japan*

Ikkou Funaki‡  
*Japan Aerospace Exploration Agency, 3-1-1 Sagami-hara, Kanagawa, 229-8510, Japan*

and

Itsuro Kimura§  
*University of Tokyo, Bunkyo-ku, Tokyo, 113-8856, Japan*

**Abstract:** An experimental study on a laser-electric hybrid thruster was conducted. A laser-electric hybrid thruster, consisting of a coaxial electrode configuration with an annular copper anode (5 and 13 mm in diameters) and a carbon fiber rod cathode (3 and 6 mm in diameters) was used to produce, laser-induced plasmas, which were accelerated by electrical means instead of direct acceleration based on only the laser ablation process. From the discharge current measurement of the laser-electric hybrid thruster, it is found that the plasma can be initiated even under low discharge voltage conditions ( $\sim 500$  V). In addition, from the thrust measurement, thrust performance showed impulse-bit of  $2 \sim 45$   $\mu\text{Nsec}$ , momentum coupling coefficient of  $5 \sim 14$   $\mu\text{Nsec/J}$ , specific impulse of  $1000 \sim 1400$  sec and thrust efficiency of  $3 \sim 5$  % for charged energies  $0 \sim 8.6$  J and a laser pulse energy of 120 mJ.

## I. Introduction

The current trend towards smaller spacecraft, which is not only mass-limited but also power-limited, has produced a strong interest in the development of micropropulsion devices.<sup>1-4</sup> The significance in reducing launch masses has attracted growing interests in regard to a decrease in mission cost and an increase launch rate. Although, in the past, many very small spacecraft lacked propulsion systems altogether, future microspacecrafts will require a significant propulsion capability in order to provide a high degree of maneuverability and capability in terms of thrust, specific impulse, or efficiency. The benefit of using electric propulsion for the reduction in spacecraft mass will likely be even more significant for mass-limited microspacecraft missions.<sup>2-4</sup> Feasibility studies of microspacecraft are currently under development for a mass less than 100 kg with an available power level for propulsion of less than 100 watts. Various potential propulsion systems for microspacecraft applications, such as ion thrusters, field emission thrusters, pulsed plasma thrusters (PPTs), vaporizing liquid thrusters, resistojets, microwave arcjets, pulsed arcjets, etc., have been proposed and are under significant development for primary and attitude control applications.<sup>4</sup>

---

\* Graduate Student, Department of Aeronautics and Astronautics, email: 6amjm014@keyaki.cc.u-tokai.ac.jp

† Associate Professor, Department of Aeronautics and Astronautics.

‡ Associate Professor, Institute of Space and Astronautical Science.

§ Professor Emeritus.

On the other hand, small onboard laser plasma thrusters are also under significant development along with the rapid evolution of novel compact laser systems. One of the advantages of such laser thrusters is that they can use any solid materials as their propellant. Therefore, the system can be very simple and small with significant controllability of thrust.<sup>5-8</sup> In order to improve the thrust performance and system simplicity of conventional electric and laser propulsion systems, preliminary studies of a laser-electric hybrid acceleration system have been conducted by the authors.<sup>9-13</sup> In this paper, we describe some of typical acceleration characteristics of the propulsion system of this type.

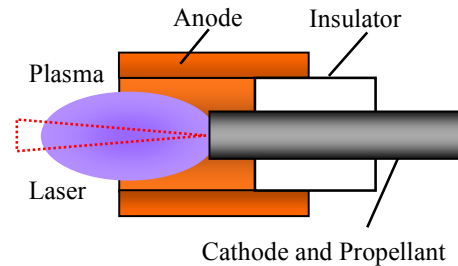
## II. Laser-Electric Hybrid Thrusters

Schematics of laser-electric hybrid acceleration systems are illustrated in Figs.1 and 2.<sup>9-13</sup> A basic idea of these systems is that laser-ablation plasma induced through laser irradiation on a solid target is additionally accelerated by electrical means. Since any solid materials can be used as propellants in these cases, no tanks, valves, or piping systems are required for the propulsion system. Therefore, the system employing these techniques can be significantly simple and compact. Because laser-ablation plasma has a directed initial velocity of tens of km/sec, which will be further accelerated by electrical means, significantly high specific impulses can also be expected.<sup>14</sup>

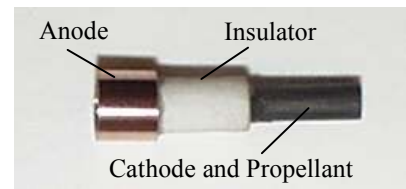
In the above hybrid cases, depending on different factors such as electrode configuration, plasma density, and electrical input power (voltage x current), acceleration mechanisms for the laser-ablation plasma can be classified into three types, i.e., i) electrostatic acceleration, ii) electrothermal acceleration, and iii) electromagnetic acceleration, as shown in Fig.3 (a),<sup>15</sup> although ii) usually occurs simultaneously with iii). Especially for laser-ablation plasma, depending on laser conditions such as pulse energy, fluence, etc., plasma density and velocity distributions can be widely controlled. Moreover, they can also be controlled through additional electric discharges.

Properly controlling a power source, or voltage and current, with optimized electrode configuration for additional electric acceleration, each acceleration mechanism can be adopted. Therefore, propulsion system that is able to satisfy all the above acceleration schemes through i) to iii) will be achieved with one thruster configuration. Namely, this system enables a robust conversion between high-specific-impulse operation and high-thrust-density operation in regard to mission requirements, as shown in Fig.3 (a). Each of two typical accelerators, a laser-electrostatic hybrid accelerator and a laser-electromagnetic hybrid accelerator, is currently under investigation and is described in the following subsections.

Regarding the forms of energy contributions, or input for acceleration, laser-electric hybrid thrusters can be classified into various operational modes as defined in Fig.3 (b). When an electric energy contribution on the acceleration process is zero compared with laser energy contribution, the thruster can be defined as being in the “pure laser propulsion mode”. If the electric contribution is smaller than the laser energy contribution, it can be defined as being in the “electric-assisted laser propulsion mode”. Also, with a greater electric contribution than the laser energy, it can be defined as being in

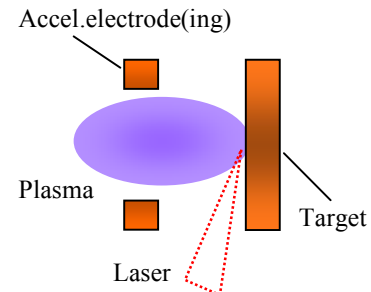


(a) Schematic illustration.

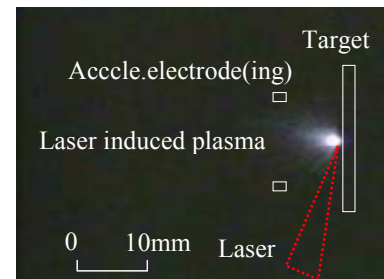


(b) Photo of the thruster.

Figure 1. Schematic illustration and photo of a coaxial laser-electromagnetic hybrid thruster.



(a) Schematic illustration.



(b) Photo of laser-induced plasma.

Figure 2. Schematic illustration and photo of a laser-electrostatic hybrid thruster.

the “laser-assisted electric propulsion mode”. Moreover, with zero contribution of lasers, it can be defined as being in the “pure electric propulsion mode”.

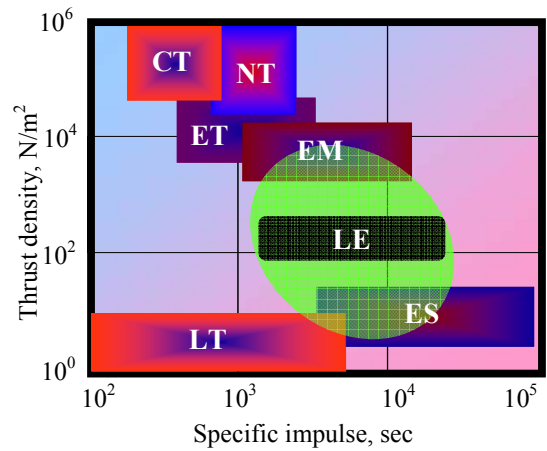
### A. Electrostatic Acceleration

One of the laser-electric hybrid acceleration regimes employed in our studies is laser-electrostatic hybrid acceleration, in which laser-ablation plasma is further accelerated by an electrostatic field.<sup>12</sup> Schematic illustration and a photograph of the accelerator are shown in Fig.1. As shown in this figure, a focused laser pulse is irradiated onto a solid target or a propellant. Then, laser-induced plasma or laser ablation is induced at an irradiated spot of the propellant surface. In the laser-ablation, first, electrons are accelerated from the surface, and then, ions are accelerated through ambipolar diffusion and Coulomb explosion. In the hybrid accelerator, such ions are further accelerated with an additional acceleration electrode. Because laser-induced plasma generated from the target surface having a directed initial velocity is further accelerated by an electrostatic field, fast ion emission and high specific-impulses can be expected.

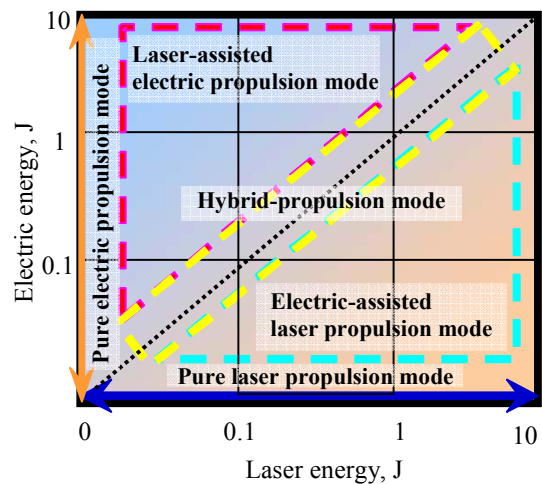
### B. Electromagnetic Acceleration

Another acceleration regime considered in this study is laser-electromagnetic hybrid acceleration.<sup>9-13</sup> Schematic of the accelerator is illustrated in Fig.2. It utilizes laser-beam irradiation to induce plasma ionized from a solid propellant between electrodes, and then an electric discharge is induced in this conductive region. As the current running between the anode and cathode is increased, the plasma can be heated and further ionized through Joule heating. Thus, the electrothermal acceleration effect becomes significant. When current exceeds more than one thousand amperes, an electromagnetic acceleration effect becomes significant. Since a primary current concentrates on the cathode center running in axial direction, a self-induced magnetic field is induced in azimuthal direction. Then a streamwise acceleration is provided through the interaction of the radial current and the azimuthal magnetic field, or Lorentz force. In addition, there is an electromagnetic pumping process wherein axial components of current cross with the azimuthal magnetic field to establish a radial gradient in the gas dynamic pressure which provides a reaction force on the cathode surface.<sup>15</sup>

Because the use of a shorter laser pulse enables a shorter pulsed-plasma generation, a significantly high peak current can be induced. Since the force induced in the accelerator is dependent on the square of the current, significant improvements in acceleration characteristics can be expected.<sup>15</sup> In addition, depending on laser power, laser-induced plasma produced from a solid propellant usually has a directed initial velocity, and this can also contribute to an improvement in the acceleration performance.



(a) Based on thrust characteristics



(b) Based on energy contribution

**Figure 3. Classification of laser-electric hybrid propulsion systems based on thrust characteristics and energy contributions, where CT: Chemical Thermal Propulsion, NT: Nuclear Thermal Propulsion, ET: Electrothermal Propulsion, EM: Electromagnetic Propulsion, ES: Electrostatic Propulsion, LT: Laser Thermal Propulsion, LE: Laser Electric Hybrid Propulsion.**

### III. Experimental Setup

In this study, two different sizes of the thrusters were examined. Sizes of the thrusters are listed in Table 1. For the thruster (Fig.1), a coaxial electrode configuration with an annular copper anode (5 and 13 mm in diameters for thrusters I and II, respectively) and a carbon fiber rod cathode (3 and 6 mm in diameters for the I and II), which is also the solid propellant, was used, in which channel lengths between the cathode edge and the anode exit were set 3 and 6 mm for the I and II, respectively. A schematic of experimental setup is given in Fig.4. A Q-sw Nd:YAG laser (BMI, 5022DNS10, wavelength:  $\lambda = 1064$  nm, pulse energy: 120 mJ and 0.7 J/pulse, pulse width: 10 nsec) was used for a plasma source. The laser pulse was irradiated into a vacuum chamber ( $10^{-3}$  Pa) through a quartz window and focused on a target, or a propellant, with a focusing lens ( $f = 100$  mm). Discharge current was monitored with a current monitor (Pearson Electronics, Model-7355, maximum current: 10 kA, minimum rise time: 5 nsec) and an oscilloscope (Tektronix TDS3034B, range: 1 nsec/div  $\sim$  10 sec/div). In this study, preliminary experiments on switching, or discharge between the cathode and anode, and discharge characteristics of the laser-induced plasma were conducted. In order to observe temporal behaviors of exhaust plasma plumes, ICCD camera observation (ANDER TECHNOLOGY, minimum gate width: 2 nsec) was conducted. Moreover, in order to estimate  $\mu$ nsec-class impulses, a calibrated torsion-balance type thrust-stand was developed and tested.<sup>15</sup> Schematic of experimental setup for impulse-bit measurement is given in Fig.5. Detailed descriptions of the thrust-stand and its calibration procedure are given in Ref.15. The balance is 450 mm long made of aluminum. Distance between the pivot and thruster is set 437 mm. For the pivots, the Flexural Pivot (SDP/SI) was used. A torsional spring rate of the pivot estimated in this case is  $k = 4.7 \times 10^{-2}$  Nm/rad. As for the displacement sensor, a non-contacting displacement sensor of eddy current type (EMIC, 503-F, NPA-010, maximum range: 1 mm, minimum displacement: 0.5  $\mu$ m) located at 450 mm from the pivots was used.

### IV. Results and Discussion

#### A. Discharge Current Characteristics

Temporal variations of discharge current for charged voltage conditions from 500 to 2,000 V and a laser pulse energy of 120 mJ for thruster I are shown in Fig.6 (a), in which a maximum charged energy is 8.65 J. In the 500 V case, a single pulse discharge peaking up to 500 A at 1.7  $\mu$ sec with a pulse width of 4  $\mu$ sec is observed. In the figure, positive values on an ordinate mean a positive current from anode to cathode. It is confirmed that electric discharges can be achieved even under low voltage conditions ( $\sim$  500

**Table 1 Sizes of thrusters**

	Anode	Cathode	Channel length
Thruster I	$\phi 5$ mm	$\phi 3$ mm	3 mm
Thruster II	$\phi 13$ mm	$\phi 6$ mm	6 mm

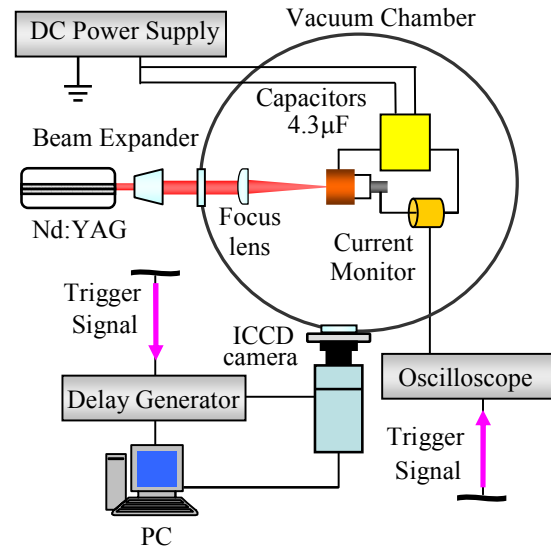


**Figure 4. Schematics of experimental setup for discharge characterization and plasma plume observation with ICCD camera.**

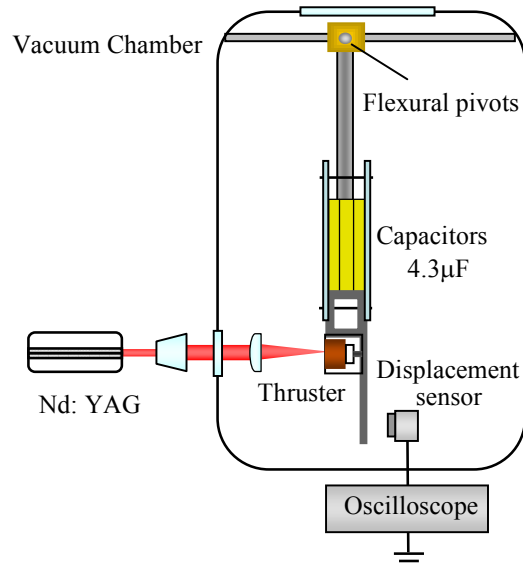
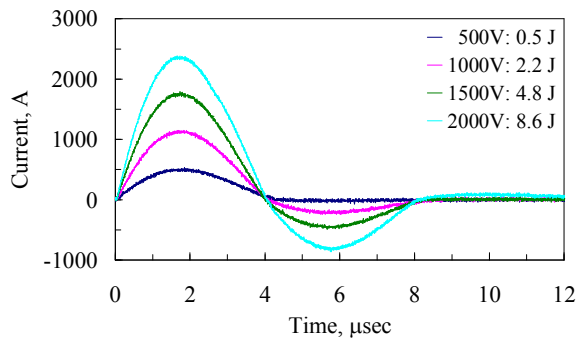


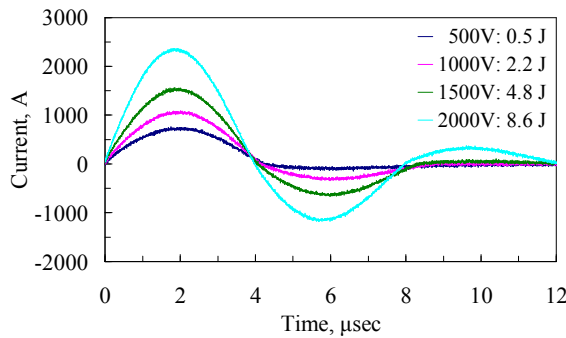
**Figure 5. Schematic of experimental setup for measurement of an impulse bit.**

V). Also, it can be seen that the higher the voltages, the higher the currents being induced. Although one positive wave of the current of about 4  $\mu\text{sec}$  duration is observed in low-voltage cases, the current oscillation with longer duration is occurring in higher voltage conditions. At 2,000 V (8.65 J), a positive peak rises up to + 2,370 A at 1.7  $\mu\text{sec}$  and converging zero at about 8  $\mu\text{sec}$ . Current waveforms for thruster II are shown in Fig.6 (b). It can be seen that the peak currents of two types of thrusters were approximately the same. At 2,000 V (8.65 J), the current abruptly rises and reaches a maximum value of + 2,340 A at 1.9  $\mu\text{sec}$ , after which it falls down to a minimum value (- 1,150 A) at 5.9  $\mu\text{sec}$  and converges zero at about 12  $\mu\text{sec}$ .

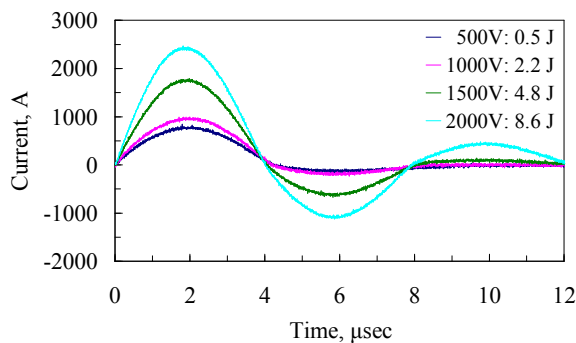
Temporal variations of discharge current are given in Fig.6 (c), where laser pulse energy of 0.7 J for thruster II is used. From the figure, the current at 2000 V (8.65 J) abruptly rises and reaches a maximum value of 2,440 A at 1.9  $\mu\text{sec}$ , after which it falls down to a minimum value (- 1,100 A) at 5.9  $\mu\text{sec}$  and converges zero at about 12  $\mu\text{sec}$ . It is confirmed that discharge current patterns did not depend on laser pulse energy.



(a) Thruster I, laser pulse energy: 120 mJ



(b) Thruster II, laser pulse energy: 120 mJ



(c) Thruster II, laser pulse energy: 0.7 J

Figure 6 Temporal variations of discharge current.

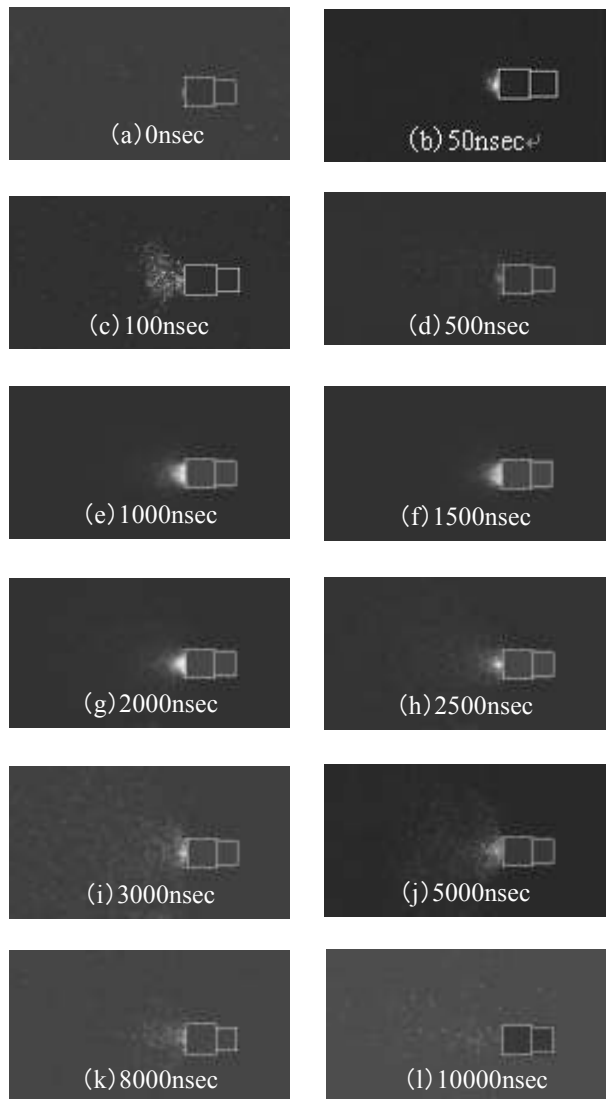


Figure 7. ICCD images of plume from thruster I for 2000 V, 4.3  $\mu\text{F}$ , 8.65 J.

## B. Plasma Plume Observation with ICCD Camera

ICCD images of a discharging plasma plume from the thruster are shown in Fig.7 for a 2,000 V case. After laser irradiation, a small-spot plasma at the center of an exposed propellant surface is induced at about 50 nsec. At 100 nsec, the plasma emission is becoming stronger. Corresponding to current wave forms of Fig.6 (a), in which the current reaches a positive peak at 1,700 nsec, a strong plasma emission is induced and the plume is rather convergent in an axial direction. At 2,500 to 3,000 nsec, the plasma plume is extending in the axial direction. Then the current reaches a negative peak at 5,000 nsec, in which the plasma emission is being stronger again. After that, the emission is gradually getting weaker scattering in the axial direction until 10,000 nsec.

## C. Thrust Performance Measurements

In Table 2, the thrust performance of pure laser propulsion mode for laser pulse energies 120 mJ and 0.7 J obtained was shown. The case of laser pulse energy for 120 mJ showed higher thrust performance than 0.7 J case.

Plots of impulse-bit measured with a torsion-balance type thrust stand for various energies charged to capacitors for laser pulse energies of 120 mJ and 0.7 J for two types of thrusters I are shown in Fig.8. As shown in this figure, impulse-bit of each thruster increases with energy of up to 8.65 J. Impulse-bits for two laser pulse energies were approximately the same. The thruster II with the larger diameter of the anode ( $\phi 13$  mm) showed higher impulse-bits than thruster I ( $\phi 5$ mm). While in terms of thrust density, the maximum value of 1.2 Nsec/m<sup>2</sup> for smaller thruster (thruster I) was larger than that of 0.3 Nsec/m<sup>2</sup> for larger thruster II. Deviations of the plots are probably due to those of laser pulse energies and misalignments of mechanical and optical elements at each operation.

Relationship between momentum coupling coefficient  $C_m$  and charged energy for laser pulse energies of 120 mJ and 0.7 J are shown in Fig.9 for thrusters I and II. From the figure the momentum coupling coefficient of each thruster gradually decreases with energy showing maximum value in the pure laser propulsion mode (Table 2). Moreover, values of the coupling coefficient for different laser energies are about the same. Regardless of the laser energies, larger coupling coefficients could be obtained with the larger thruster.

For the mass measurement we used an electronic precision balance (Shimazu AUX220, minimum mass 0.1 mg). The typical number of pulse-shots to measure the mass show was 500 times. The mass in this case was 2.3 mg for a charged energy of 8.65 J and a laser pulse energy of 120 mJ with thruster II. Mass shots with charged energy 2.2 ~ 8.6 J for thrusters I and II are shown in Table 3. It is apparent that the mass shots of two thrusters I and II for a laser pulse energy of 120 mJ were approximately the same (Table 3). From these results, specific impulse for each plot of impulse-bit was estimated. In Fig.10, specific impulse variations with charged energy for laser pulse energies of 120 mJ and 0.7 J for two types of thrusters are plotted. It is found that the thruster II for a laser pulse energy 120 mJ showed higher specific impulse than thruster I. Since the thruster II for laser pulse energy 0.7 J showed a larger mass shot than that of 120 mJ, it showed a lower specific impulse than the case of 120 mJ. This is probably due to the thermal loss of a propellant. Specific impulse

**Table 2 Thrust performance of pure laser propulsion mode**

Table 2 Thrust performance of pure laser propulsion mode		
Thruster II		
Laser pulse energy	120 mJ	0.7 J
Propellant	Carbon fiber	
Mass shot	0.04 $\mu$ g	0.76 $\mu$ g
Impulse-bit	2 $\mu$ Nsec	7 $\mu$ Nsec
Momentum coupling coefficient	14 $\mu$ Nsec/J	9 $\mu$ Nsec/J
Specific Impulse	4400 sec	900 sec
Thrust efficiency	31%	4%

**Table 3 Mass shot measurements**

Table 3 Mass shot measurements			
Thruster I			
Laser pulse energy	120 mJ		
Charged energy	2.2 J	4.9 J	8.6 J
Mass shot	1.6 $\mu$ g	2.7 $\mu$ g	4.2 $\mu$ g
Thruster II			
Laser pulse energy	120 mJ		
Charged energy	2.2 J	4.9 J	8.6 J
Mass shot	1.7 $\mu$ g	3.0 $\mu$ g	4.8 $\mu$ g
Laser pulse energy	0.7 J		
Charged energy	2.2 J	4.9 J	8.6 J
Mass shot	2.6 $\mu$ g	3.6 $\mu$ g	5.4 $\mu$ g

of lower laser energy case gradually decreases with increasing charge energy. On the other hand, specific impulse of higher laser pulse energy case is almost constant with charge energy. The values of specific impulse of thruster II for charged energy 2 ~ 5 J is higher than conventional PPTs operated under similar energy levels. For a higher charged energy, it is hence confirmed that part of propellant is consumed by the discharge, which may not effectively contribute to impulse-bit.

Relationship between thrust efficiency ( $= (\text{kinetic energy}) / [(\text{charged energy}) + (\text{laser energy})]$ ) and charged energy for laser pulse energies of 120 mJ and 0.7 J for two types of thrusters are given in Fig.11. As shown in this figure, thrust efficiency decreases with increasing charged energy for each thruster. At charge energies of 5 to 9 J for thruster II, there are no big differences in the efficiencies between different laser energies. Some values of the thrust efficiency obtained in this study for input energy ranging 5 ~ 9 J are lower than those of conventional PPTs.<sup>11</sup> This is probably due to structure of the thruster. When the channel length of the thruster is not long enough, all the charged energy may not be discharged. Some fraction of the mass shot may not be able to receive an acceleration force and namely not contributing to induction of the impulse resulting in the mass loss.

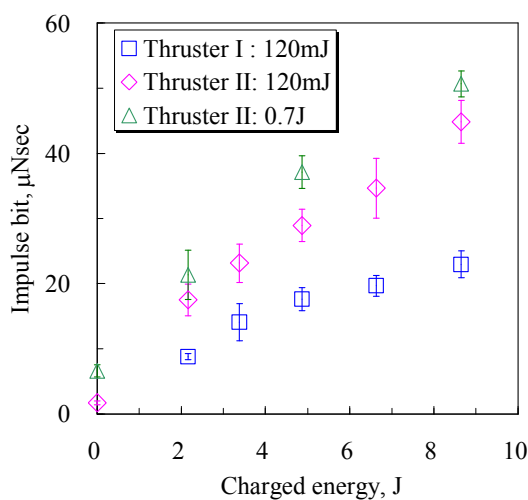


Figure 8. Impulse bit vs. charged energy.

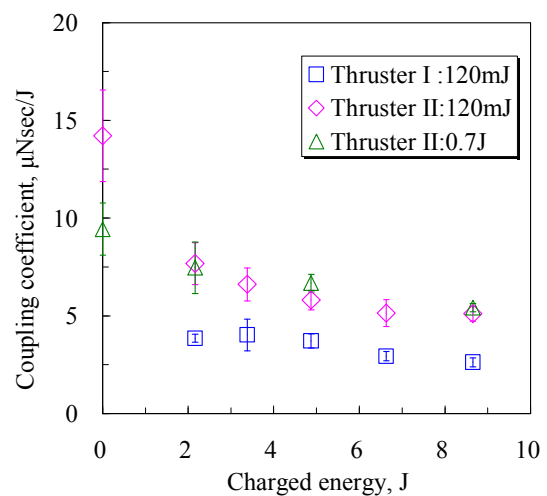


Figure 9.  $C_m$  vs. charged energy.

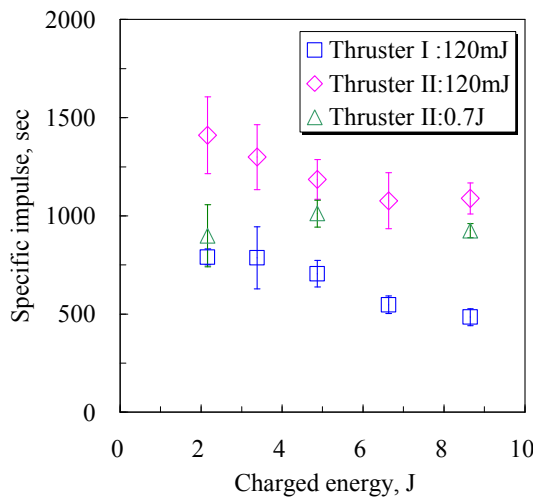


Figure 10. Specific impulse vs. charged energy.

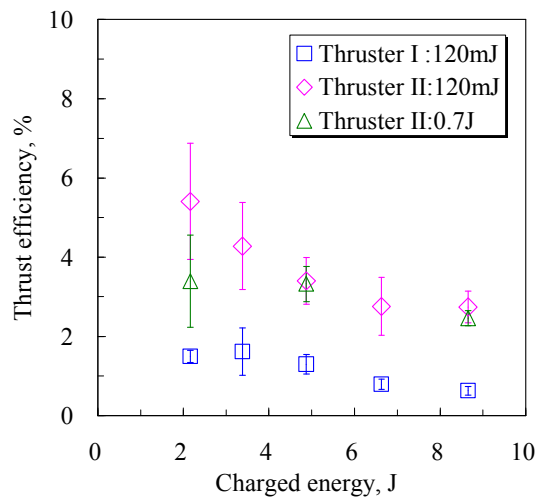


Figure 11. Thrust efficiency vs. charged energy.

## V. Conclusions

A fundamental study on laser-electric hybrid thruster was conducted, in which laser-induced plasmas were generated through laser-beam irradiation on to a solid target and accelerated by electrical means instead of direct acceleration using only a laser beam. For two different sizes of the thruster, a feasibility study on electromagnetic acceleration mode of the laser ablation plasma was conducted.

Following results were obtained.

- I. Electric discharges can be achieved even under low voltage conditions ( $\sim 500$  V).
- II. From the plasma behavior observations with the ICCD camera, it was shown that intense plasma emission and oscillating peak currents were simultaneously occurring, showing effects of the currents on plasma emission, or namely acceleration.
- III. Impulse-bit of two cases of laser pulse energy (120 mJ and 0.7 J) were approximately same. Most portion of the plasma induced through laser ablation is supplied to a discharge channel as a propellant with the directed initial velocity in a short duration ( $\sim 500$  nsec) before main discharge occurring at  $1 \sim 1.7$   $\mu$ sec, and leads the discharge. So the laser-ablation plasma with directed initial velocity of tens of km/sec may not be effectively accelerated by the Lorents force.
- IV. It is remarkable that specific impulse and thrust efficiency are high for relatively low charged energies below 5 J. In this low charged energy cases, it is confirmed that the laser-electric hybrid thruster can suppress the mass shot, leading to high specific impulse operation of the thruster.

## References

- <sup>1</sup>Myers, R.M., et al., "Small Satellite Propulsion Options," AIAA Paper 94-2997, June 1994.
- <sup>2</sup>Mueller, J., "Thruster Options for Microspacecraft: A Review and Evaluation of Existing Hardware and Emerging Technologies," AIAA Paper 97-3058, July 1997.
- <sup>3</sup>Leifer, S., "Overview of NASA's Advanced Propulsion Concepts Activities," AIAA Paper 98-3183, July 1998.
- <sup>4</sup>Micci, M. M., and Ketsdever, A. D. (ed.), Micropropulsion for Small Spacecraft (Prog. Astronautics and Aeronautics 187), American Institute of Aeronautics and Astronautics, 2000.
- <sup>5</sup>Phipps, C., and Luke, J., "Diode Laser-Driven Microthrusters: A New Departure for Micropropulsion", AIAA Journal, Vol.40, No.2, 2002, pp.310-318.
- <sup>6</sup>Gonzales, D., and Baker, R., "Micropropulsion using a Nd:YAG Microchip Laser," Proceedings of SPIE Vol.4760, pp.752 – 765, 2002.
- <sup>7</sup>Pakhomov, A.V., et al., "Specific Impulse Study of Ablative Laser Propulsion," AIAA Paper 2001-3663, 2001.
- <sup>8</sup>Horisawa, H., and Kimura I., "Fundamental Study on Laser Plasma Accelerator for Propulsion Applications," Vacuum, Vol.65 (No.3-4), pp.389-396, 2002.
- <sup>9</sup>Jahn, R.G., Physics of Electric Propulsion: McGraw-Hill, 1968, pp.198-316.
- <sup>10</sup>Martinez-Sanchez, M., and Pollard, J. E., J. Propulsion and Power 14, pp.688-699 (1998).
- <sup>11</sup>Burton, R. L., and Turchi, P. J., J. Propulsion and Power 14, pp.716-699 (1998).
- <sup>12</sup>Horisawa, H., et al., Beamed Energy Propulsion: AIP Conference Proceedings Vol.664, 2003, pp.423-432.
- <sup>13</sup>Horisawa, H., et al., IEPC 2003-75 (2003).
- <sup>14</sup>Kawakami, M., et al., AIAA Paper 2003-5028 (2003).
- <sup>15</sup>Kawakami, M., et al., Proc. Asian Joint Conf. on Propulsion and Power 2004, pp.419 – 424 (2004).